Phonon mechanism for the evaporation of clusters

D. I. Zhukovitskiĭ

Institute of High-Temperature, Russian Academy of Sciences, 127412 Moscow, Russia

Using the methods of molecular dynamics, we investigate the evolution of a cluster in a supersaturated vapor at constant temperature and pressure. We observe instability in the size of the cluster, and claim that the mechanism for evaporation of atoms from the cluster surface is a collective process related to phonon creation. In the phonon spectrum we observe period doubling, which is characteristic of a strange attractor. © *1996 American Institute of Physics.* [S1063-7761(96)01003-0]

1. INTRODUCTION

In the classical theory of nucleation[1,4] it is assumed that the mechanism for evaporation from the surface of a seed of the liquid phase (a cluster) located in a supersaturated vapor is single-particle-like, as in the case of a planar liquid surface. The atom that evaporates is one that acquires sufficient kinetic energy as a result of random collisions with its neighbors to overcome a potential barrier of constant height equal to the heat of evaporation. In point of fact, however, the heat of evaporation is not a fixed quantity for a cluster containing only a few dozen atoms. If phonons are excited in the cluster (by phonons we mean certain types of collective oscillations with specific energy and wavelengths much larger than the mean distance between atoms, by analogy with liquids), then the interatomic distance, and with it the heat of evaporation, will oscillate. Since the probability of evaporation of an individual atom depends exponentially on the heat of evaporation, this probability is large during that phase of the oscillations where the interatomic distance is large, and small in the opposite case. The rate of evaporation, in turn, determines the critical size of a cluster which leaves it in a state of unstable equilibrium with the supersaturated vapor, i.e., the quantity on which the rate of homogeneous nucleation depends.

Since model representations[5,8] are useful only for discussing the thermodynamic properties of clusters, the only method that allows us to study the evaporation mechanism "from first principles" is the method of molecular dynamics. In these discussions we cannot confine ourselves to the microcanonical Gibbs ensemble, which is traditional in molecular dynamics (see, e.g., Refs 9–11), since this system is not realistic enough. In fact, the equilibrium in this case is stable and is determined by the conditions

$$\left(\frac{\partial s}{\partial g}\right)_{E,V,N} = 0, \quad \left(\frac{\partial^2 s}{\partial g^2}\right)_{E,V,N} < 0,$$

where s is the entropy, g is the number of atoms in the cluster, and E, V, and N are the energy, volume, and particle number, respectively. Equilibrium is reached via the exchange of atoms between the cluster and the vapor. In contrast, for real systems it is the pressure P and the temperature T that are fixed rather than E, V, and N, which corresponds to the conditions for quasistationary nucleation.[4] A cluster in supersaturated vapor turns out to be unstable against an increase (or decrease) in size, and its critical parameters are determined by the different conditions:[3]

$$\left(\frac{\partial \phi}{\partial g}\right)_{P,T,N} = 0, \quad \left(\frac{\partial^2 \phi}{\partial g^2}\right)_{P,T,N} < 0,$$

where ϕ is the thermodynamic Gibbs potential. Therefore we must simulate a (P,T) ensemble instead of a (E,V) ensemble. In this case, the rate of evaporation can be determined along with an estimate of the critical size. Furthermore, it is interesting to compare this estimate with the results of calculations based on thermodynamic models of nucleation (see, e.g., Ref. 8).

In order to realistically simulate the vapor surrounding the cluster, in our studies we introduce a spherical cell with transparent boundaries, so that vapor atoms that reach this surface exit the system. At the same time, this boundary is a source of atoms, which are randomly generated over the entire surface of the cell in such a way that the cell is filled with gas with the Maxwellian velocity distribution corresponding to the given constant temperature and pressure. The evolution of the size of a cluster placed at the center of the cell is determined by the processes of evaporation and condensation of atoms on its surface.

The study of collective vibrations of clusters yields important information about their properties, in particular about the mechanism of evaporation. A vibration connected with oscillations in the average distance between atoms in a cluster, which in the literature are called "breathing" vibrations, were studied for solid argonlike clusters both theoretically[12,14] and experimentally.[15] A radical change in the cluster phonon spectrum occurs when it melts. In order to study the spectrum of vibrations of a liquid cluster, we analyzed the potential energy per individual atom in the cluster. This quantity is proportional to the "instantaneous" heat of evaporation, and therefore directly determines the flux of atoms evaporating from the cluster surface (i.e., the evaporation rate). The fundamental result of this paper is the identification of a unique relation between the spontaneous appearance of "breathing" vibrations and a sharp increase in the rate of evaporation of a liquid cluster, which indicates that the mechanism for evaporation is collective, or phonon-mediated. Note that our use of the term "phonon mecha-

nism'' here implies that we can describe the evaporation as a consequence of the interaction of cluster atoms while in thermal motion. Independent of the simulation conditions, the phonon spectra typically exhibit sharp maxima with frequency doubling. This shows that the liquid cluster is an example of a dynamic system with the properties of a strange attractor.

The system under study and the numerical methods for simulation are described in Sec. 2, the results of the simulation of the instability in the cluster size in Sec. 3. In Sec. 4 we analyze the phonon spectrum of clusters, and the results discussed in Sec. 5.

2. SIMULATION METHOD

The system under study consists of a cluster located at the center of a cell and the surrounding supersaturated vapor. In order to model a vapor at constant pressure and temperature, it is not necessary to rigorously fix these quantities by introducing additional terms into the Hamiltonian of the system and impose kinematic coupling conditions, as is normally done in molecular dynamic methods.[16] It is sufficient to fix only the average number of vapor atoms in the cell N_v, and assume that the temperature T_0 is a constant parameter. Then the corresponding (Maxwellian) velocity distribution of vapor atoms within the cell is ensured by choosing suitable boundary conditions.

Let us assume that such a condition is the generation of a flux at the boundary equal to the one-sided atomic flux through an arbitrary surface in the equilibrium gas. In this case, for simplicity we will assume that the vapor density is sufficiently small that we can treat the vapor as ideal and neglect atomic collisions. Then $P = k_B T_0 n_v$, where k_B is Boltzmann's constant, $n_v = N_v/V$ is the concentration, V is the cell volume, and the single-particle distribution function $f(t,\mathbf{r},\mathbf{v})$ is described by the Boltzmann equation $\partial f/\partial t + \mathbf{v}\nabla f = 0$ with the initial condition $f(0,\mathbf{r},\mathbf{v}) = 0, |\mathbf{r}| < R$, where R is the cell radius (the coordinate origin is located at its center). We write the boundary condition in the form $f(t,\mathbf{R},\mathbf{v}) = f_0(v)$ for $v_n < 0$, where $v_n = \mathbf{v}\mathbf{R}/R$ is the normal component of the velocity, $\mathbf{R}$ is the radius vector of a point at the surface of the cell. From the solution of the kinetic equation

$$f(t,\mathbf{r},\mathbf{v}) = \begin{cases} 0, & t < \tau_r, \\ f_0(v), & t \geq \tau_r, \end{cases} \qquad (1)$$

where $v\tau_r(\mathbf{r},\mathbf{v}, R) = \rho + \sqrt{\rho^2 + R^2 - r^2}$, $\rho = \mathbf{v}\mathbf{r}/v$, it is clear that a Maxwell distribution is established in the cell if we choose $f_0(v) = (n_v/\pi^{3/2}u^3)\exp(-v^2/u^2)$, where $u^2 = 2k_B T_0/M$ and M is the mass of an atom, and remove those atoms with $v_n > 0$ that intersect the surface from the system. In this case, the time it takes to fill the cell with vapor is $\tau_r \propto R/u$. Consequently, we require that the flux of atoms generated at the surface with velocities lying in the interval $(v_k, v_k + dv_k)$, $k = x, y, z$ be

$$dJ = -v_n f_0(v) dv_x dv_y dv_z. \qquad (2)$$

In the generation process, we first randomly choose a point on the surface, and then generate three components of velocity with the probability distribution $p(v_k)$

$= (1/\pi^{1/2}u)\exp(-v_k^2/u^2)$. If in this case it turns out that $v_n < 0$, an atom is added to the system with probability $p_n = -4\pi v_n \tau n_v R^2/k_r$. After one time step τ this procedure is repeated k_r times (we took $k_r = 2$). Obviously this generation process can be considered quasicontinuous if $p_n \sim 4\pi u \tau n_v R^2/k_r \ll 1$. It is not difficult to see that the flux of atoms

$$dJ = p(v_x)p(v_y)p(v_z)p_n dv_x dv_y dv_z k_r/4\pi\tau R^2$$

coincides with (2) in this case.

Let us consider the procedure for assembling the initial cluster. Since the internal structure of the cluster is close to that of a liquid under these conditions, it is reasonable to construct the initial cluster out of a simple cubic lattice for which the coordination number is closer to the number established by numerical modeling than for a close-packed lattice. The cluster is built out of shells, such that the coordinates of the j-th atom located in the l-th shell satisfy the condition $x_j^2 + y_j^2 + z_j^2 = la^2$, where x_j/a, y_j/a, and z_j/a are integers, a is the lattice period, $l = 0,1,...$ The shells are filled sequentially until the desired number of atoms in the cluster is reached. For each atom we generate three velocity components with the distribution $p(v_k)$. We then subtract the velocity components of the center of mass, which is located at the center of the cell, from these velocity components.

The interaction potential of the atoms is chosen to be of Lennard–Jones 12-6 form: $u(r_{ij}) = 4\epsilon[(\sigma/r_{ij})^{12} - (\sigma/r_{ij})^6]$, where $r_{ij} = |\mathbf{r}_i - \mathbf{r}_j|$, and $\mathbf{r}_{ij}$ are the radius vectors of atoms. Furthermore, we add an additional force to the force acting on an atom, which simulates the interaction of the cluster with a heat bath. The role of the latter may be played by, e.g., a buffer gas. The need to introduce this force, which stabilizes the cluster temperature, is dictated by the fact that large temperature fluctuations can qualitatively change the character of the cluster evolution. In the absence of a heat bath, each evaporation (condensation) event at the cluster surface causes a change in its temperature $\delta T \sim 2q/3gk_B$, where q is the heat of evaporation. Since $q/k_B T_0 \gg 1$, we may have

$$\frac{q\delta T}{k_B T_0^2} = \frac{2q^2}{3gk_B^2 T_0^2} > 1$$

even for $\delta T/T_0 \ll 1$. This means that the rate of evaporation, which is proportional to $\exp(q\delta T/k_B T_0^2) \gg 1$, undergoes large-amplitude fluctuations, i.e., we cannot define an average temperature $\langle T \rangle$ for the cluster (the angle brackets denote averaging over time). In this case, a strong correlation exists between the processes of evaporation and condensation. Thus, in the absence of a heat bath the evolution of the cluster is determined not only by the quantity $\langle T \rangle$ but also by the fluctuation amplitude δT; furthermore, $\langle T \rangle$ differs from the vapor temperature (see Sec. 3). Therefore the temperature T_0 is not a good thermodynamic parameter for this system, and in order to simulate the (P,T) ensemble we must reduce the level of temperature fluctuations; this is why we have introduced the interaction with a heat bath.

The interaction term is written in the form of a frictional force, and the equation of motion for the jth atom in the cluster has the form

$$\ddot{\mathbf{r}}_j = \frac{1}{\tau_0^2} \sum_{i \neq j} \left[2\left(\frac{\sigma}{r_{ij}}\right)^{14} - \left(\frac{\sigma}{r_{ij}}\right)^8 \right] (\mathbf{r}_j - \mathbf{r}_i)$$
$$+ \frac{1}{\tau_f}\left(\sqrt{\frac{T_0}{T}} - 1 \right)\dot{\mathbf{r}}_j, \qquad (3)$$

where $\tau_0 = \sigma\sqrt{M/24\epsilon}$ is the time scale for the molecular dynamics, τ_f is the temperature relaxation time, and

$$T = \frac{M}{3gk_B} \sum_{j=1}^{g} \mathbf{v}_j^2$$

is the "instantaneous" cluster temperature, defined by using the equipartition theorem[16] (in equilibrium this would be $\langle T \rangle = T_0$). The second term on the right side of (3) corresponds to acceleration of atoms for $T < T_0$ and braking of these atoms in the opposite case. Obviously this term must be small enough compared to the first term that atomic vibrations do not degenerate into aperiodic motion. On the other hand, it must be large enough that the temperature fluctuations are small, $q\,\delta T/k_B T_0^2 < 1$. Thus, the quantity τ_f must be chosen to ensure a compromise between these cases. Since the atoms of vapor are generated by the heat bath itself, whose state does not depend on the state of the cluster, we set $\tau_f = \infty$ for these atoms.

In order to identify which atoms belong to the cluster and which belong to the vapor, we adopt the following widely used criterion: an atom is assumed to belong to the cluster if it has even a single neighbor at a distance smaller than r_b. In Refs. 17 and 18 it was shown that this criterion works well for amorphous clusters; the number of atoms in the cluster depends weakly on r_b if $r_b \sim \sigma$. In this paper, we choose r_b from the condition of minimum fluctuations of g; under the conditions described in Sec. 3, $r_b = 1.434\sigma$.

In order to compensate for the drift of the cluster from the center of the cell due to Brownian motion, we shift the cell to the cluster center of mass $\mathbf{r}_{cm}$ as soon as we find that $r_{cm}^2 \geq R^2/12$. This corresponds to a transformation of coordinates and velocities $\mathbf{r}'_j = \mathbf{r}_j - \mathbf{r}_{cm}$, $\mathbf{v}'_j = \mathbf{v}_j$, i.e., a shift of the coordinate origin that does not affect the motion of the atoms that make up the cluster. The vapor atoms that happen to be outside the new cluster ($|\mathbf{r}'_j| > R$) are reflected in a centrosymmetric fashion with respect to the point $\mathbf{r}_{cm}/2$: $\mathbf{r}'_j = -\mathbf{r}_j$, $\mathbf{v}'_j = -\mathbf{v}_j$. In this case, we conserve the number of vapor atoms moving within the cell and toward its surface, and also the total number of particles in the system.

The introduction of a cell actually implies a cutoff in the potential. The results of Refs. 19 and 20, where the simulation was carried out by the method of molecular dynamics for a planar boundary between vapor and liquid in an argon-like system, indicate that the saturated vapor pressure differs considerably from the real pressure, even for a cutoff radius equal to 3σ. Therefore the radius R must be quite large; in this paper we took $R = 8\sigma$. In this case, the condition for quasicontinuity of the generation $p_n \ll 1$ is still satisfied.

3. INSTABILITY AND CRITICAL SIZE

The system of equations (3) was numerically integrated with step size $\tau = 0.05$ (the time was varied in units of τ_0).

The optimum value of T_0 was found to be the melting temperature of real argon:[21] at higher temperatures, the vapor was nonideal, while at lower temperatures it was impossible to compare the numerical results with calculations based on other nucleation theories. If we use the widely adopted value $\epsilon = 119.4$ K (see Ref. 16), then $T_0 = 0.7017\epsilon$. The average value of the number of vapor atoms in the cell, which was kept constant in the course of each process, was chosen according to the degree of supersaturation $S = n_v/n_s(T_0)$, where $n_s(T_0) = 2.4 \cdot 10^{-3}\sigma^{-3}$ is the concentration of saturated vapor.

In order to test our procedure for generating vapor atoms at the walls of the cell, we calculated the temperature

$$T_v = \frac{M}{3N_v k_B} \left\langle \sum_{j=1}^{N_v} \mathbf{v}_j^2 \right\rangle,$$

the concentration $\langle N_v \rangle/V$, and the compressibility factor for the vapor

$$\frac{PV}{\langle N_v \rangle k_B T_v} = 1 - \frac{1}{3\langle N_v \rangle k_B T_v} \left\langle \sum_{i<j} r_{ij} \frac{du}{dr_{ij}} \right\rangle \qquad (4)$$

when $S = 4$ in the absence of a cluster. The generation continued up to a time 10^4. The derived value of T_v exceeded T_0 by 4%, and the concentration turned out to be 5% lower than n_v (when we "turned off" the interaction of the vapor atoms, this difference went to 0.1%). The value of the compressibility factor we found was 0.95, i.e., somewhat larger than that of real argon. This is due to the presence of dimers in the latter; under our conditions, the dimer fraction is of order 0.1.[21] Thus, the algorithm described in Ref. 2 for generation of vapor atoms allows us to simulate the vapor with satisfactory accuracy at a prespecified pressure and temperature.

Further calculations were performed for cells containing a cluster. At $t = 0$ the original cluster is created, and the generation of vapor begins. The process ends as soon as either a shrinking cluster completely disappears, or the number of atoms in it doubles. Two types of numerical experiments were carried out, corresponding to $\tau_f = 0.125$ and $\tau_f = \infty$. Their results were quite different. Thus, for the first type the average value of the temperature pulsations δT did not exceed 2 to 3 K (the condition for weakness of the interaction with the heat bath $\delta T \tau_0/2T_0\tau_f \ll 1$ was satisfied in this case). For the second type $\delta T \sim 20-30$ K, so that it was difficult to assign a definite temperature to the system. One consequence of the strong correlation between evaporation and condensation events mentioned in Sec. 2 is an order-of-magnitude increase in the time it takes for a cluster to completely disappear when $\tau_f = \infty$. This feature was used as a way to minimize the loss of clusters to evaporation at the beginning of the process, when the cell is filled with vapor: for $t < \tau_r \approx 65$ we set $\tau_f = \infty$ in the first variant as well.

We performed a series of experiments with $S = 4.4$ and various initial values of the number of atoms in the cluster $g(0)$. Typical time dependences for the first type of simulation illustrate the phenomenon of size instability well (Fig. 1). Depending on the initial size of the cluster, we can distinguish two groups of clusters: those for which $g(0) < g^*$,
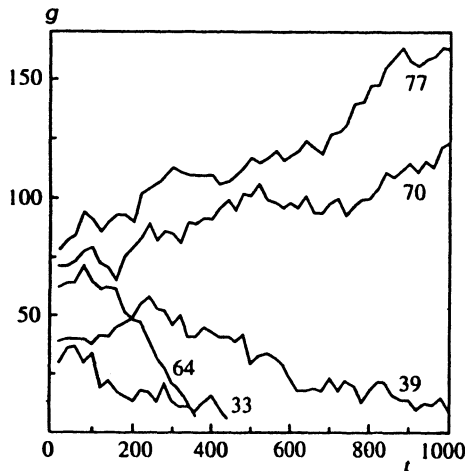
FIG. 1. Time dependence of cluster size for various initial sizes (shown at the right of each curve).

which decrease in size and disappear completely after a certain time, and those for which $g(0) > g^*$, which grow without bound. Here $g^* \cong 60$. Clusters with initial sizes $g^* \pm 7$ are randomly assigned to one of these two groups.

Let us estimate the magnitude of the cluster size fluctuations. According to the classical theory of nucleation,[4] a cluster executes a random walk in the "size" space. If we assume that this random walk is due only to fluctuations in n_v, we find that it corresponds to a diffusion coefficient of the same order as the frequency of condensation events ν at the cluster surface. Therefore, the size difference between two initially identical clusters is $\delta g \sim \sqrt{2 \nu t}$. For $t = 10^3$ we find that $\delta g \sim 10$. In order to explain the discrepancy in the observed growth and disappearance times for the clusters (Fig. 1), the quantity δg must be several times larger. Consequently, the fluctuations in cluster size are determined by fluctuations in the rate of evaporation, which have a large value even for small δT.

It is clear from Fig. 1 that subcritical clusters, rather than beginning to shrink, grow until a certain time t_{max} is reached, despite the fact that for $t < \tau_r$ the vapor concentration is less than its steady-state value (see the curves for $g(0) = 39$ and 64). The quantity t_{max} varies from 80 to 350 for various realizations. For a constant value of S the flux of condensing atoms is constant as well. Consequently, when $t < t_{max}$ the rate of evaporation is significantly higher. As we show in the next section, at the maximum of the function $g(t)$ an abrupt restructuring of the cluster phonon spectrum occurs.

We investigated the dependence of the critical size on the degree of supersaturation for values of S from 3.8 to 5.0. It turned out that the classical theory of nucleation[1-4] gave values of g^* that were 2 to 3 times smaller than the numerical models. The formal use of the Tolman size correction, which reduces the surface tension of the cluster by a factor of $1 + 2(g^*)^{-1/3}$ compared to the planar surface of a liquid, gives the unphysical result $g^* = 1$. The theory of nucleation with size corrections[8] leads to the opposite conclusion that the effective surface tension for an argonlike cluster is larger than for a planar surface; therefore, the critical size turns out to be larger than for the classical theory of nucleation. Cal-

culations based on the model of Ref. 8 give values of g^* that are 25 to 30% lower than those obtained from numerical simulation.

In the second type of simulation ($\tau_f = \infty$), a shrinking of the clusters is observed for all sizes below the spinodal, i.e., for $S < 10$. For $S > 10$, independent of the initial sizes, the clusters grow. It is noteworthy that their average temperature $\langle T \rangle$ was found to be 4 to 5% lower than T_v. During the period when the temperature fluctuations were positive, the probability of evaporation increased considerably; evaporation of dimers and trimers was observed. Thus feature of the evolution is in agreement with the known experimental fact that nucleation is hindered in the absence of a buffer gas.

For $g < 40$, the frequency of escape from the cluster surface increases considerably for clusters containing up to 10 to 12 atoms; we saw this happen in both types of simulations. In fact, the smallest size coincided with the critical size in the denser vapor, where the equilibrium concentration of small clusters was no longer negligible. From the principle of detailed balance it follows that the fraction of light clusters must also increase during evaporation. Two consecutive escape phases of a ten-atom cluster are shown in Figs. 2a and 2b.

In all realizations we observed three types of vibration: single-particle vibrations of atoms in their cells; bulk ("breathing") vibrations connected with oscillations of the interatomic spacing (Figs. 2c and 2d); and surface vibrations analogous to capillary waves on the surface of the liquid (Fig. 2e). Note that the latter type of vibration, for which deformation of the cluster is characteristic at a constant average interatomic spacing, appears only as the cluster melts. Figure 2f shows a highly excited state in its "inhaling" phase; note the threadlike structures.

Various types of vibrations appear at different times after the process begins. Thus, single-particle vibrations appear immediately, surface vibrations after a time of order 20. It is very significant that for $t < t_{max}$ not a single realization exhibits bulk oscillations. This leads us to believe that there is a connection between these types of vibrations and the rate of evaporation. In order to study it we analyzed the phonon spectra.

4. PHONON SPECTRA OF CLUSTERS

The quantity that is most suitable for analyzing collective vibrations is the potential energy per cluster atom referenced to the temperature:

$$U(t) = (g k_B T_0)^{-1} \sum_{i < j} u(r_{ij}).$$

On the one hand, this quantity is very sensitive to oscillations of the interatomic spacing, while on the other hand it differs very little from the quantity $q/k_B T_0$ that determines the rate of evaporation. The spectra of $U(t)$ were analyzed for 45 realizations in which the initial number of atoms in a cluster was 42 for each of the simulation types. All of the features we will discuss below are more or less evident in each realization and are illustrated with one example. The functions $U(t)$ and $g(t)$ are shown in Fig. 3. Point A is the start of the
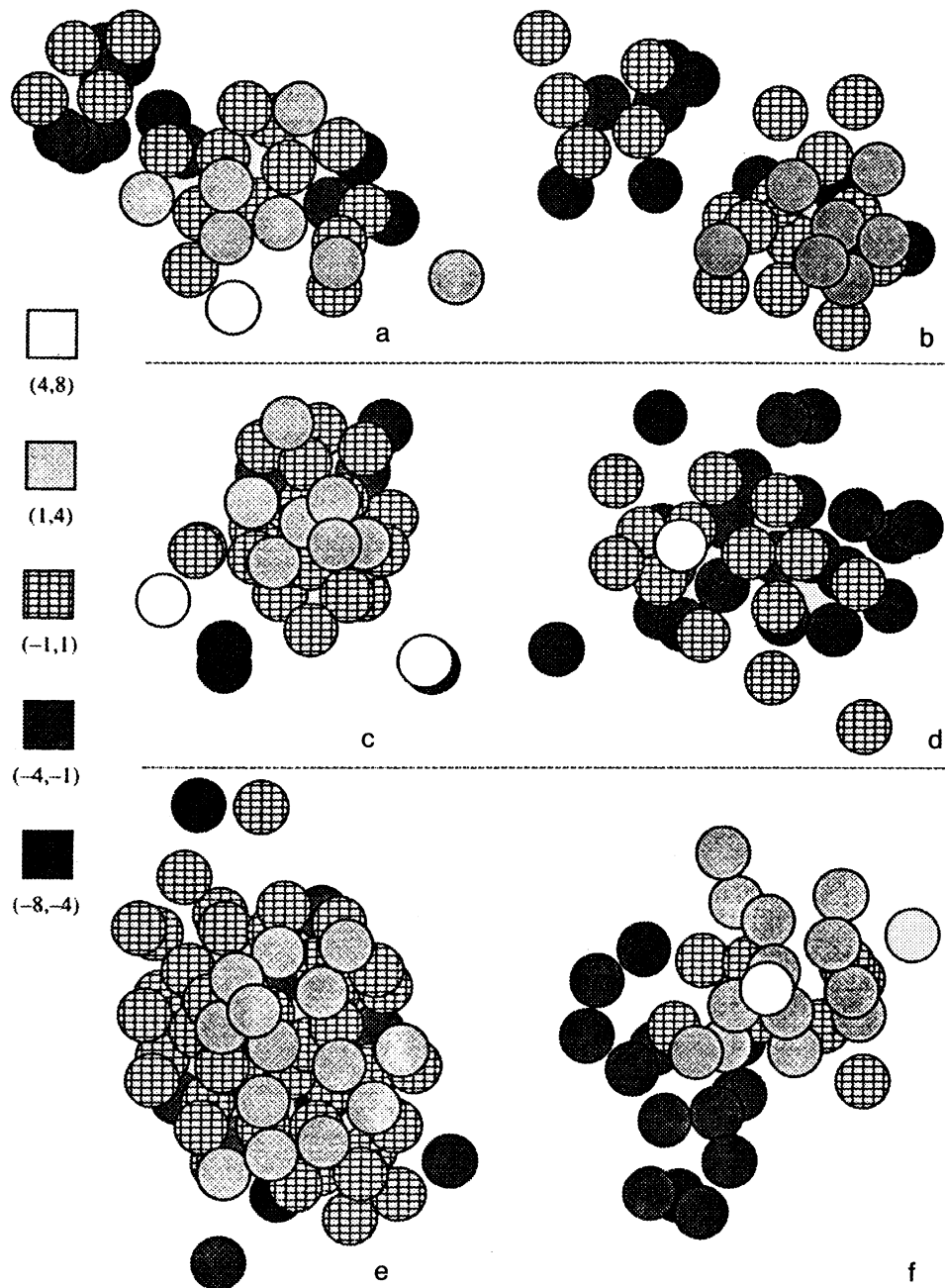
FIG. 2. Phases in the evolution of clusters: a,b—evaporation of a ten-atom cluster; c,d—"exhaling" and "inhaling" phases of collective oscillations separated by a time equal to 24; e—lower mode of surface oscillations, $t = 19.5$; f—highly excited state with threadlike structures. The degree of shading corresponds to the range of atomic coordinates (shown on the left) along the axis perpendicular to the plane of the figure.

process, point C the time at which the cluster size has decreased by two. At point B there is a significant change in the character of the oscillations—a sharp increase in amplitude and a longer period. From Fig. 3 it is clear that $t_B = t_{max} = 153$ coincides with the delay time for the beginning of rapid evaporation (the reason for nonmonotonicity of $g(t)$ when $320 < t < 427$ is discussed in Sec. 5). The same regularities are also observed when $\tau_f = \infty$, but on a different time scale: for the realization chosen here, $t_B = t_A = 440$; we took $t_C - t_B = 630$.

There is a significant systematic trend in the function $U(t)$, which must be removed before beginning the spectral analysis. To do this, we write the quantity being analyzed in the form of a trend and a rapidly oscillating component: $U = \bar{U} + \tilde{U}$. The trend is specified by a broken line consisting of linear functions over time intervals much smaller than

$t_C - t_B$ but much larger than the characteristic oscillation period. On each interval coefficients for these functions are determined using the method of least squares with additional continuity conditions at the interval boundaries.

A distinctive feature of this process is its nonstationary behavior; therefore, in postulating ergodicity we must characterize its time time-dependent spectral functions. To do so we need the additional assumption that these functions vary sufficiently slowly on the time scale θ we used to calculate and average them, i.e., we use the approximation of a local spectral density. In this approximation the spectral density of the quantity $\bar{U}$ is defined by the average

$$G(\omega) = \langle |\tilde{U}_\omega|^2 \rangle \equiv \theta^{-1} \int_t^{t+\theta} |\tilde{U}_\omega(t')|^2 dt',$$
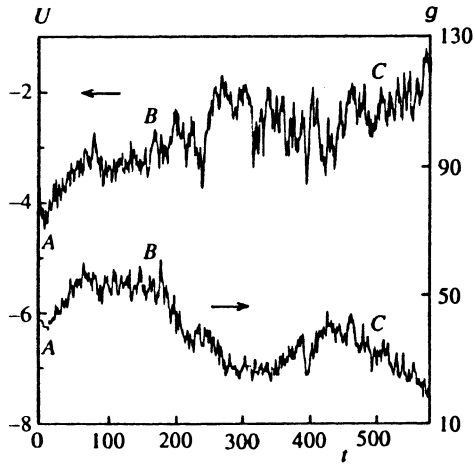
FIG. 3. Potential energy per atom and cluster size versus time; $S=4.4$, $\tau_f=0.125$.

where

$$\widetilde{U}_\omega(t)=t_1^{-1}\int_t^{t+t_1}\widetilde{U}(t')\exp(i\omega t')dt',$$

$$\omega=2\pi k/t_1, \quad k=1,2,\dots \tag{5}$$

is the coefficient of the finite Fourier transform on the interval $(t,t+t_1)$; the values of k are bounded from above by $k\leq\omega_{max}t_1/2\pi$, where ω_{max} is a prespecified maximum frequency. In order to decrease the step in ω when we calculate $G(\omega)$, the length of the interval t_1 on which the Fourier coefficients are found was varied over the limits $\theta/2<t_1<\theta$ with a step $\tau_\omega=0.5$ chosen such that the resolution of this method $\delta\omega=(16\pi/3)(\tau_\omega/\theta^2)$ was much smaller than $\omega_{min}=2\pi/\theta$, i.e., the minimum frequency that coincides with the half-width of the spectral lines. The line broadening is natural and is caused by the finiteness of the cluster lifetime (formally, the finiteness of the length of the computation interval for $G(\omega)$). In other words, each Fourier coefficient is computed for a given t_1 and k at different times t' on the interval $(t,t+\theta)$, and then the square of its modulus is averaged on this interval. Note that the decay time of the autocorrelation function $\xi(t)$ for the quantity $\widetilde{U}$ is found to be large—at least it is no smaller than the lifetime of the cluster. Therefore, the commonly used expression

$$G(\omega)=\lim_{\theta\to\infty}\left[\frac{2}{\theta}\int_0^\theta\xi(t)\cos(\omega t)dt\right].$$

is inapplicable here.

In analyzing the results of our numerical experiments we assumed that the spectral density changes abruptly at the point B and is constant over the intervals AB and BC; the corresponding values of θ are $(t_B-t_A)/2$ and $(t_C-t_B)/2$. Figures 4 and 5 show the vibration spectra $G_1(\omega)$ and $G_2(\omega)$ for the first and second intervals respectively, with additional smoothing of the spectra:

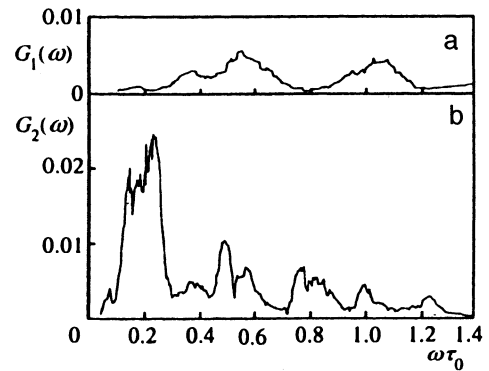$$G_{1,2}(\omega)=(2\,\delta\omega)^{-1}\int_{\omega-\delta\omega}^{\omega+\delta\omega}G(\omega')d\omega'.$$

FIG. 4. Spectral density of the quantity $\widetilde{U}(t)$ on intervals AB (a) and BC (b), with $\tau_f=0.125$.

The different characteristics of the oscillations over these two intervals are clearly evident in the spectra (see parts a and b in Figs. 4 and 5). Figures 4b and 5b show the behavior of the sharp maxima (peaks) at frequencies much smaller than the single-particle frequencies. The fact that the spectra and evaporation rate change abruptly at $t=t_B$ suggests that these phenomena are related.

5. DISCUSSION

In the low-frequency range we can distinguish three peaks in Figs. 4b and 5b at frequencies $\omega\tau_0=0.14, 0.24, 0.48$, and $0.11, 0.24, 0.45$ respectively. The fact that the spectra of these two realizations, which correspond to different conditions and have different "ages," are in such close agreement (the two largest peaks in Fig. 4b are poorly resolved due to the large natural broadening) indicates that they have the same origin. Since the quantity $\widetilde{U}(t)$ is most sensitive to oscillations in the interatomic spacing, we can interpret these peaks as the onset of "breather" vibrations, or phonons. We also cannot rule out the contribution of surface oscillations, because they are strongly coupled to the bulk oscillations. Actually, in all the realizations a stretched-out shape of the cluster (Figs. 2c, 2d) corresponds to a "breathing-out" phase, whereas a flattened shape (Fig. 2e) corresponds to a "breathing-in" phase. This correspondence contradicts what happens in solid clusters.[12] Note that the dependence of the peak positions on the cluster size is quite weak–the corre-
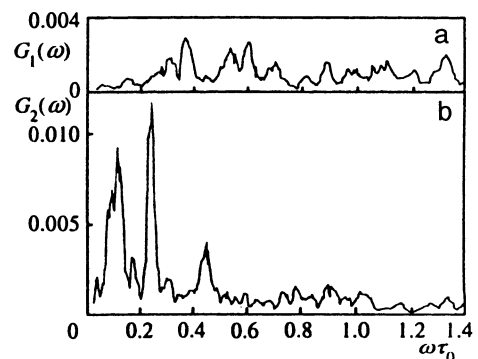

FIG. 5. The same function as in Fig. 4, for $\tau_f=\infty$.

sponding broadening does not exceed the natural broadening. The change in the spectra observed for clusters that are shrinking with $g < g^*$ takes place for growing clusters as well, where $g > g^*$. Since the evaporation rate is related not only to the presence of phonons but also to the cluster size, decreasing with increasing g, the connection between phonons and changes in the cluster dimension is not unambiguous in general and can be clearly discerned only for rather small clusters.

The following pattern is worth noting: the frequencies corresponding to the peaks discussed above are found to be in the approximate ratios $1 : 2 : 4$. These are characteristic not of a succession of harmonics (in this case we would expect 1:3:5) but rather of a strange attractor.[22] Let us list the facts that argue in favor of this system having a strange attractor: 1) period doubling, 2) a sharp "catastrophic" change in the spectrum at $t = t_B$, 3) a decay mechanism for the onset of chaos, connected with pumping of energy from higher to lower frequencies in the spectrum. The latter feature is characteristic, e.g., of turbulent flow. The spectrum of pulsations in velocity in a shear layer[23], for example, is very similar to what we have found in this work.

Let us discuss the mechanism for energy pumping in our system when $\tau_f = \infty$. Obviously, the mechanism is sustained oscillation, with the role of an energy source played by the generation of atoms at the surface of the cell. Pumping of energy takes place when atoms condense on the cluster surface. As our observations show, the clusters are such "loose" formations that an atom arriving at the surface will, as a rule, stick to it. In this case it executes several oscillations with decreasing amplitude, giving up energy to neighboring atoms. This is a single-particle process, and the corresponding frequencies are the same order of magnitude as the high frequencies of single-particle vibrations. The dissipation mechanism is connected with evaporation of the atoms—at each evaporation event an energy of order q is lost. However, evaporation is a collective process, for which low frequencies are characteristic. Thus, pumping of energy takes place between the single-particle and phonon frequencies, giving rise to a characteristic spectrum with frequency doubling. At finite but rather long τ_f the interaction with the heat bath does not distort this picture.

Our results lead us to one unconditional conclusion: namely, that the increase in the rate of evaporation of atoms from a cluster surface is connected with the appearance of vibrations with frequencies of order $(0.1 - 0.5)\tau_0^{-1}$. The amplitude of the oscillations $U(t)$ for these vibrations reaches $2 k_B T$ (Fig. 3); therefore, the probability of evaporation of an individual atom in the "breathe-in" phase (Fig. 2d) is several times that in the "breathe-out" phase (Fig. 2c). This

indicates a collective mechanism for evaporation. The fact that clusters grow with time for $t > t_B$ (Fig. 3) does not contradict this conclusion. In fact, the deformation of the cluster in the "breathe-out" phase is larger the larger the vibration amplitude. For $t = 282$ the cluster is so distended that the ratio of longitudinal size to transverse reaches 4. In this case the phonon decays, since all the atoms of the cluster are converted to surface atoms. For repeated apparition of the phonon and establishment of an evaporation rate connected with it we require times of order 10^2, during which the cluster grows.

The basic patterns we observed in these numerical experiments can be described as follows. The rate of evaporation of a cluster, fluctuations in its size, and its critical size are all connected with the presence of phonons. The spectrum of vibrations of a thermally excited cluster exhibits period doubling, which is characteristic of a strange attractor. We claim that these results are not specific to argon. If we are right, then liquid-metal clusters should also exhibit an increased rate of evaporation and an abrupt decrease in the rate of nucleation when the phonons interact with a resonant electromagnetic field.

[1] R. Becker and W. Döring, Ann. Phys. **24**, 719 (1935).
[2] M. Fol'mer, *Kinetics of Formation of a New Phase* [in Russian], K. M. Gorbunova and A. A. Chernov (eds.), Nauka, Moscow (1986).
[3] Ya. I. Frenkel', *Kinetic Theory of Liquids: Collected works* [in Russian], Akad. Nauk SSSR, Moscow–Leningrad (1959).
[4] Ya. B. Zel'dovich, Zh. Éksp. Teor. Fiz. **12**, 525 (1942).
[5] H. Reiss, A. Tabazadeh, and J. Talbott, J. Chem. Phys. **92**, 1266 (1990).
[6] H. M. Ellerly and H. Reiss, J. Chem. Phys. **97**, 5766 (1992).
[7] C. L. Weakliem and H. Reiss, J. Chem. Phys. **101**, 2398 (1994).
[8] D. I. Zhukovitskii, J. Chem. Phys. **101**, 5076 (1994).
[9] J. K. Lee, J. A. Barker, and F. F. Abraham, J. Chem. Phys. **58**, 3166 (1973).
[10] D. J. McGinty, J. Chem. Phys. **58**, 4733 (1973).
[11] A. I. Rusanov and E. Brodskaya, J. Colloid and Interface Sci. **62**, 542 (1977).
[12] Y. Ozaki, M. Ichihashi, and T. Kondow, Chem. Phys. Lett. **182**, 57 (1991).
[13] R. E. Allen, G. P. Aldredge, and F. W. de Wette, Phys. Rev. B **4**, 1661 (1971).
[14] K. Kobashi and R. D. Etters, Surf. Sci. **150**, 252 (1985).
[15] U. Buck and R. Krohne, Phys. Rev. Lett. **73**, 947 (1994).
[16] D. W. Heermann, *Computer Simulation Methods in Theoretical Physics*, 2nd ed., Springer-Verlag, New York (1990).
[17] K. Binder, J. Chem. Phys. **63**, 2265 (1975).
[18] M. Rao, B. J. Berne, and M. Kalos, J. Chem. Phys. **68**, 1325 (1978).
[19] M. J. P. Nijmeijer, A. F. Bakker, C. Bruin, and J. Sikkenk, J. Chem. Phys. **89**, 3789 (1988).
[20] M. J. Haye and C. Bruin, J. Chem. Phys. **100**, 556 (1994).
[21] N. V. Vargaftik, *Handbook of Thermophysical Properties of Gases and Liquids* [in Russian], Nauka, Moscow (1972).
[22] M. I. Rabinovich, Usp. Fiz. Nauk **125**, 123 (1978) [Sov. Phys. Usp. **21**, 443 (1978)].
[23] H. Sato, J. Fluid Mech. **44**, 741 (1970).